



## Review

## Molecular mechanism of Thioflavin-T binding to amyloid fibrils

Matthew Biancalana<sup>a,b</sup>, Shohei Koide<sup>c,\*</sup><sup>a</sup> Laboratory of Immunology, National Institute of Allergy and Infectious Diseases, National Institutes of Health, Bethesda, MD 20892, USA<sup>b</sup> Centre for Protein Engineering, Medical Research Council Centre, Hills Road, Cambridge CB2 0QH, UK<sup>c</sup> Department of Biochemistry and Molecular Biology, The University of Chicago, 929 East 57th Street, Chicago, IL 60637, USA

## ARTICLE INFO

## Article history:

Received 24 February 2010

Received in revised form 1 April 2010

Accepted 7 April 2010

Available online 22 April 2010

## Keywords:

Cross-beta

Amyloid dye

Protein design

Molecular dynamics simulation

Molecular recognition

Self-assembly

## ABSTRACT

Intense efforts to detect, diagnose, and analyze the kinetic and structural properties of amyloid fibrils have generated a powerful toolkit of amyloid-specific molecular probes. Since its first description in 1959, the fluorescent dye Thioflavin-T (ThT) has become among the most widely used “gold standards” for selectively staining and identifying amyloid fibrils both *in vivo* and *in vitro*. The large enhancement of its fluorescence emission upon binding to fibrils makes ThT a particularly powerful and convenient tool. Despite its widespread use in clinical and basic science applications, the molecular mechanism for the ability of ThT to recognize diverse types of amyloid fibrils and for the dye's characteristic fluorescence has only begun to be elucidated. Here, we review recent progress in the understanding of ThT–fibril interactions at an atomic resolution. These studies have yielded important insights into amyloid structures and the processes of fibril formation, and they also offer guidance for designing the next generation of amyloid assembly diagnostics, inhibitors, and therapeutics.

© 2010 Elsevier B.V. All rights reserved.

## 1. Introduction

Amyloid fibrils are insoluble proteinaceous materials found in a wide range of protein-misfolding diseases, including Alzheimer's and prion diseases as well as several types of systemic amyloidoses [1,2]. In 1853, Virchow described among the first methods for the detection of amyloid by staining diseased organ samples with an iodine-sulphuric acid treatment [3,4]. Because the insoluble nature of amyloid fibrils has precluded the use of many biochemical tools, amyloid dyes have since served as the dominant method for amyloid investigation.

Throughout the early and mid 20th century, the histological detection of amyloid was commonly performed using Congo red, a deep crimson dye adapted from the fabric industry. Unfortunately, the Congo red staining process is laborious and requires the use of polarized light microscopy, and the dye's enigmatic “apple green birefringence” is often difficult to interpret [5]. The so-called direct dyes, represented by Congo red, function based on different affinities to fibrils and non-fibrillar materials. Their use requires staining followed by washing, leading to significant level of background staining as well as low reproducibility. In contrast, fluorogenic compounds become highly fluorescent only when they are bound to a particular molecular entity, and thus they offer a set of highly sensitive and convenient techniques for detecting cellular components and structures beyond those observable with direct dyes [6]. In

1959, Vassar and Culling demonstrated the potential of fluorescent microscopy for amyloid fibril diagnosis in a pioneering report of amyloid-specific stains. They were first to describe the use of the benzothiazole dye Thioflavin-T (ThT) as a potent fluorescent marker of amyloid in histology (Fig. 1a) [7]. They noted that ThT selectively localized to amyloid deposits, thereupon exhibiting a dramatic increase in fluorescent brightness (Fig. 1b and c). In comparisons against several routine amyloid dyes, they recommended ThT be used for the “demonstration of amyloid, it being far superior to Congo red or methyl violet” [7].

Research conducted in the late 1980s and early 1990s was critical in expanding the range of applications of ThT from histology to *in vitro* characterization. Naiki et al. and LeVine [8–13] were among the first to thoroughly characterize the fluorescence spectra and binding properties of ThT. They demonstrated that, upon binding of fibrils, ThT displays a dramatic shift of the excitation maximum (from 385 nm to 450 nm) and the emission maximum (from 445 nm to 482 nm) and that ThT fluorescence originates only from the dye bound to amyloid fibrils [8,11]. The several orders of magnitude increase in ThT fluorescence intensity upon fibril binding makes it an unusually sensitive and efficient reporter, thus eliminating the need for washing and enabling real-time, in-solution observation of fibrillization (Fig. 1d and e) [14]. Its high solubility in water and moderate affinity to fibrils ( $K_d$  in the sub- and low- $\mu$ M range) additionally make ThT amenable to many experimental systems [15]. Importantly, these studies demonstrated that ThT binds equally effectively to many fibrils prepared from synthetic and biological sources [8,11]. These results provided critical support to the growing view that amyloid fibrils shared a common molecular structure and bolstered the use of peptide models for studying amyloid fibrils.

\* Corresponding author.

E-mail address: [skoide@uchicago.edu](mailto:skoide@uchicago.edu) (S. Koide).

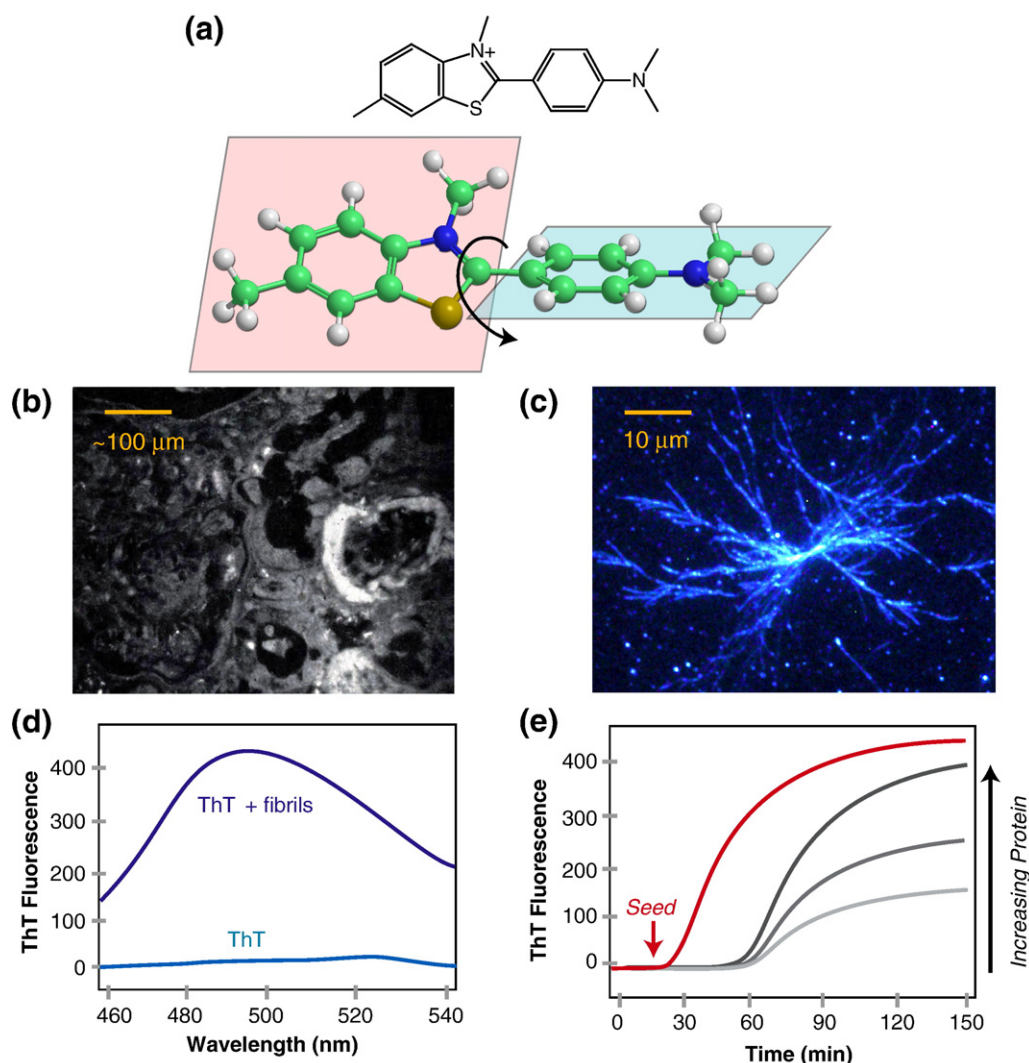


**Fig. 1.** Common experimental techniques employing ThT. (a) Structure of ThT (top). The two planer segments of ThT whose mutual rotation defines its chirality are also shown (bottom). (b) Early histology using Thioflavin-T to stain primary kidney amyloid [7]. (c) TIRF microscopy image of branched glucagon fibrils stained with ThT [21]. (d) Characteristic increase in ThT fluorescence upon binding to amyloid fibrils. (e) Fibrillization kinetics of increasing concentrations of a fibril-forming peptide, monitored by ThT fluorescence. The rapid onset of fibrillization induced through seeding is also shown. Images in b and c have been reproduced with permission.

Amyloid fibrils are characterized by a long, generally unbranched ribbon-like morphology [16]. At the molecular level, amyloids share a common “cross- $\beta$ ” architecture, consisting of laminated  $\beta$ -sheets whose strands run perpendicular to the long-axis of the fibril (Fig. 2a) [16]. This  $\beta$ -rich composition produces the characteristic 4.8 Å and 10–11 Å reflections observed in X-ray diffraction experiments of amyloid fibrils, which are attributed to the strand spacing within and between  $\beta$ -sheet layers, respectively [16,17]. It has become clear that many polypeptides have an inherent ability to self-associate into  $\beta$ -rich fibril structures, explaining the broad incidence of pathogenic amyloids [18]. Interestingly, the cross- $\beta$  architecture is also shared by “functional amyloids” that play key roles in bacterial, fungal, and animal cells [19,20]. The studies by Naiki et al. and LeVine showed that dye binding is linked to the presence of the cross- $\beta$  structure of fibrils. This realization was a critical turning point in the use of amyloid dyes not merely as indicators of the presence of mature amyloids, but as a tool for dissecting their structure and the mechanism of amyloid formation. For example, a combination of ThT staining and total internal reflection fluorescence (TIRF) microscopy has recently allowed real-time visualization of fibril morphology changes and revealed a previously uncharacterized branched morphology (Fig. 1c) [21]. The ability of ThT and its derivatives to specifically recognize and bind with modest affinity to amyloid has allowed it to serve as an

excellent starting scaffold for derivatization and elaboration to generate a number of alternative amyloid stains and clinical reagents, including for use in medical imaging of amyloid in living patients [22–24]. A large number of these ThT derivatives have been developed and reviewed elsewhere [22].

ThT is perhaps the most widely used amyloid dye among the hundreds of amyloid reports published yearly. The intensive use of ThT as an *in vitro* marker of amyloid formation has spawned substantial research into the mechanism of ThT binding, with the main goal of answering the following questions:

1. What common structure(s) does ThT recognize and how?
2. How do these interactions lead to the dramatic increase in ThT fluorescence?

Within the past several years, a series of critical experimental analyses of ThT have illuminated many of the detailed and atomic-level interactions necessary for ThT binding and fluorescence. Because several recent reports have discussed the broad range of amyloid dyes [15,25,26], here we focus on recent atomic-level studies of the fibril-binding mechanism of ThT. Through a combination of biophysical and biochemical analysis, protein engineering, fluorescence microscopy, and computational simulation, a coherent mechanism for ThT–fibril interactions has emerged.

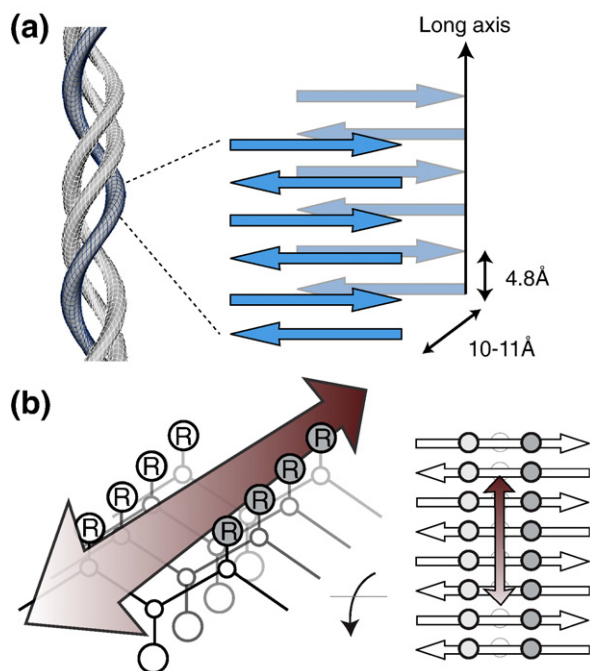


**Fig. 2.** The common structure of fibrils and a structural rationale for fibril–ThT interactions. (a) Cross- $\beta$  structure of amyloid fibrils, formed from layers of laminated  $\beta$ -sheets. (b) “Channel” model of ThT binding to fibril-like  $\beta$ -sheets. ThT is proposed to bind along surface side-chain grooves running parallel to the long axis of the  $\beta$ -sheet.

### 1.1. Spectroscopic characteristics of ThT bound to fibrils

Fluorescence enhancement upon binding to fibrils is the most defining and thoroughly studied property of ThT. It is believed that the dramatic increase in ThT fluorescence results from the selective immobilization of a subset of ThT conformers [27,28]. A wealth of experimental data and quantum mechanical predictions suggests that ThT behaves as a “molecular rotor” [29,30]. In solution, a low-energy barrier allows the benzylamine and benzathiole rings of ThT to rotate freely about their shared carbon–carbon bond (Fig. 1a). This rotation rapidly quenches excited states generated by photon excitation, causing low fluorescence emission for free ThT (Fig. 1d). In contrast, rotational immobilization of ThT preserves the excited state, resulting in a high quantum yield of fluorescence (Fig. 1d). By extension, amyloid fibrils are likely to present a ThT-binding site that sterically “locks” the bound dye, thus leading to an enhancement of ThT fluorescence.

In addition to its fluorescent properties, circular dichroism (CD) spectra of ThT bound to fibrils often display a substantial “Cotton effect” peak at 450 nm that reflects the dye’s twisted, chiral conformation [27,28,31] (Fig. 1a). However, it does not appear that immobilizing ThT in a chiral conformation is necessary for a large fluorescence enhancement. For instance, a crystallographic study showed that ThT bound to acetylcholinesterase is in an achiral, planar conformation (Fig. 3), even though the dye exhibits a high level of fluorescence indistinguishable from ThT bound to fibrils [32]. Taken together, these results suggest that the chiral twist of ThT is a consequence of ThT binding to a chiral environment of amyloid fibrils but not a prerequisite for a large enhancement of ThT fluorescence.

### 1.2. Channel model of ThT binding

The increasing number of structural models for amyloid fibrils has provided a molecular foundation for rationalizing the binding modes of ThT. ThT binds to diverse fibrils, despite their distinct amino acid sequences, strongly suggesting that ThT recognizes a structural feature common among fibrils. Because amyloid fibrils share the cross- $\beta$

architecture, it is generally accepted that the surfaces of cross- $\beta$  structures form the ThT-binding sites. The cross- $\beta$  structure of fibrils (Fig. 2a) gives rise to a specific arrangement of side-chains termed “cross-strand ladders” presented on the  $\beta$ -sheet framework (Fig. 2b) [33]. These cross-strand ladders consist of repeating side-chain interactions running across  $\beta$ -strands within a  $\beta$ -sheet layer (i.e. parallel to the long axis of the fibril) and arise from the inherently repetitive nature of self-assembly. Recent structures of short fibril-forming peptides demonstrate that neighboring rows of cross-strand side-chains occur regardless of peptide sequence, and that these side chains form extended channel-like motifs along solvent-exposed surfaces of fibrils into which linear dyes could bind (Fig. 2b) [34–37]. Thus, ThT binding to the  $\beta$ -sheet surface along channels formed by cross-strand ladders would rationalize the ability of ThT to bind many peptide self-assemblies.

Using polarized fluorescence microscopy, Krebs et al. [38] revealed that ThT molecules bound to fibrils are aligned parallel to the long axis of the fiber. Importantly, the cross-strand ladders are also aligned parallel to the long-axis of the fiber, and thus these results provided among the earliest evidence that the regular orientations of side chains in fibrils might be the common recognition motif underlying ThT’s broad range of amyloid staining. However, the resolution of fluorescence microscopy is insufficient for elucidating atomic details of ThT–fibril interactions. A similar channel model for large, linear dyes such as Congo red was suggested as early as 1974 [39,40].

### 1.3. Self-association models of ThT binding

Alternate theories of ThT binding have emphasized the capacity of ThT for self-association. Khurana et al. [41] noted that most experiments employing ThT are performed at or above the critical micelle concentration (CMC) of the dye, estimated at  $\sim 4 \mu\text{M}$  in water. They therefore hypothesized that amyloid staining by ThT is largely the result of hydrophobic interactions between amyloid and ThT micelles. However, subsequent reports have argued that the CMC under similar conditions is  $\sim 30 \mu\text{M}$ , and thus micelles should not exist under commonly used ThT concentrations [31]. A more nuanced emerging theory proposed by Groenning et al. [42,43] suggests that ThT may bind as excited dimers (“excimers”) to large hydrophobic cavities within fibrils. However, none of these alternative models can fully account for the chiral bias of bound ThT [27,28] nor its preference to bind parallel to the long axis of fibrils [38]. Moreover, analysis of ThT binding cooperativity suggests that independent ThT molecules often bind at a single type of site [13]. While the self-association models may explain some aspects of promiscuous ThT staining, they are inconsistent with numerous recent works detailing specific molecular interactions of ThT with the fibril surface.

## 2. Atomic level studies of ThT–fibril interactions

There remains a paucity of experimental data that has directly determined the modes of fibril–dye interactions at an atomic level. Fibrils and other peptide self-assemblies are insoluble and often heterogeneous in their composition, making it extremely difficult to characterize their interactions with ligands using high-resolution techniques such as X-ray crystallography and solution NMR spectroscopy. Moreover, the modest affinity of these dyes to fibrils can impede the collection and interpretation of biophysical data. Thus, there have been no experimental structures of ThT or any other dyes bound to fibrils. The approaches to surmount these experimental obstacles have been two-fold: *in silico* simulation of ThT binding, and the application of smaller and more experimentally amenable self-assembly model systems. Both methodologies have yielded considerable insight into the ThT binding mechanism and defined the minimal requirements for ThT-binding competent surfaces.



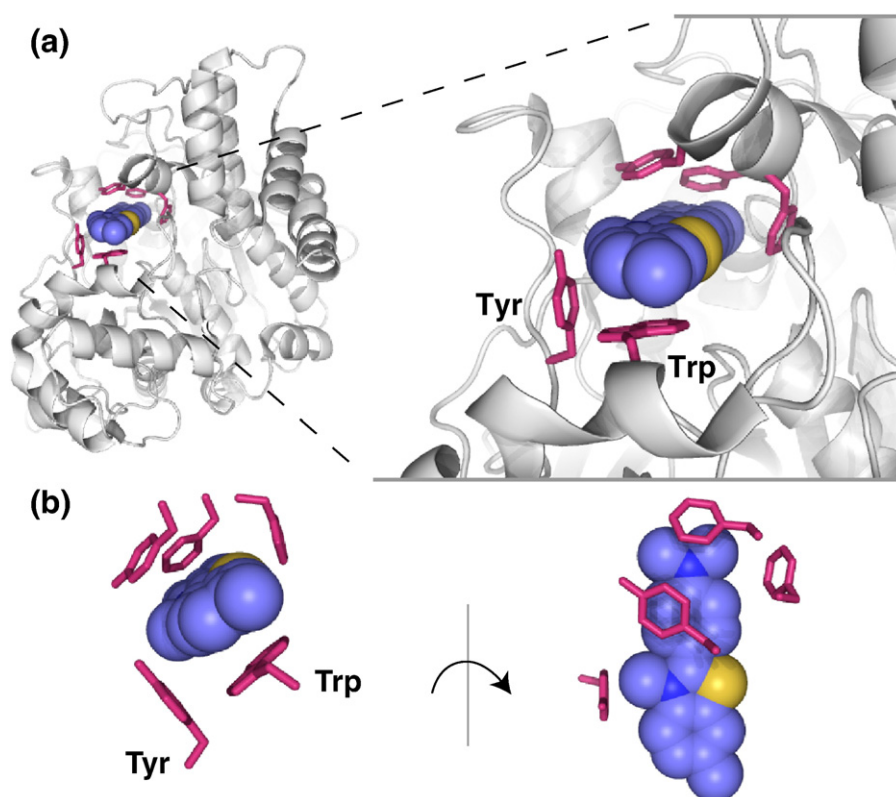


**Fig. 3.** Crystal structure of ThT bound to acetylcholinesterase (PDB 2J3Q) [32]. (a) Acetylcholinesterase is shown in cartoon representation, colored gray. All residues within 4 Å of ThT are shown as red sticks, except for Tyr121, which is omitted for clarity. The aromatic residues (Tyr and Trp) forming ThT-binding surfaces similar to that observed in the PSAM are labeled. The carbon, nitrogen and sulfur elements of ThT are in lavender, blue, and yellow, respectively. (b) The ThT-binding pocket of acetylcholinesterase shown in orthogonal views, with the protein main-chain atoms omitted.

### 2.1. Molecular dynamics simulations demonstrate ThT binds in side-chain channels

Computational simulations allow structurally complex amyloid fibrils to be dissected into tractable minimalist models that effectively eliminate uncontrollable assemblies plaguing experimental studies. Wu et al. [44,45] have extensively investigated the mechanistic basis of amyloid-dye interactions using this molecular dynamics simulation strategy (Fig. 4a and b). For their simulations, Wu et al. [44,45] constructed eight-stranded segments of bi-layer cross- $\beta$  protofibrils of the peptide sequence KLVFFAE based on the atomic structures of short fibril-forming peptides. Because amyloids are structurally repetitive, even a small  $\beta$ -sheet segment can effectively capture the properties of a much larger fibril superstructure. These simulations thus allowed Wu et al. to examine ThT-binding to three common motifs in fibril-like structures: exposed  $\beta$ -sheet edges, an extended  $\beta$ -sheet surface, as well the laminated “steric zipper” interface between the  $\beta$ -sheets. ThT-binding was performed by placing the protofibril models in a periodic water box with ~9100 water molecules, four ThT molecules, and four neutralizing chloride ions. Molecular dynamics simulations were conducted at 320 K over 20 ns, and the resulting bound populations of ThT clustered in order to reveal preferential sites for dye-interactions.

The results from the ThT simulations have provided strong support for the channel model, demonstrating that linear dyes bind parallel to the long axis of the fibril surface in grooves formed by side-chain ladders (Fig. 2a and b) [44,45]. Interestingly, binding between the sheets was rarely observed, presumably because the stability of the hydrophobic steric zipper present between  $\beta$ -sheets precluded intercalation of dye. Interactions with the edges of the sheet were also less common than those observed along the flat  $\beta$ -sheet surface. Furthermore, ThT was found to rapidly bind and dissociate from the

fibril surface, in agreement with the moderate  $K_d$  of amyloid dyes. Among the most striking insights was the observation that ThT did not bind uniformly to the  $\beta$ -sheet surface, but preferentially interacted with channels formed by aromatic residues (for instance, a Val-Phe cross-strand motif; Fig. 4a and b). These results demonstrate that there exist punctuated sites with high ThT affinity in amyloid fibrils. Thus, surface-exposed grooves lined with aromatic amino acids may be a common element among many fibrils that can be stained with ThT.

### 2.2. Peptide self-assembly mimics (PSAMs) experimentally define a minimalist ThT binding site

In a parallel series of experiments, Biancalana et al. [46] designed a set of novel ThT-binding proteins to define the minimal requirements for ThT binding. These proteins were based on the peptide self-assembly mimic (PSAM) model system (Fig. 4c) [46], which are highly stable, monomeric, and water-soluble recombinant proteins. The PSAMs are derived from *Borrelia* outer surface protein A (OspA), which contains a flat single-layer  $\beta$ -sheet capped at either end with globular domains [47]. The ThT-binding proteins were designed using a PSAM scaffold in which three copies of an endogenous  $\beta$ -hairpin were copied and re-inserted into the central  $\beta$ -sheet, thus forming a sheet with four homologous  $\beta$ -hairpins comprising eight  $\beta$ -strands (i.e. “OspA + 3bh”) [47]. The PSAMs capture the fundamental, repetitive features of a fibril-like  $\beta$ -sheet surface in a water-soluble protein that is easily adapted to biophysical analysis including X-ray crystallography. Importantly, the PSAMs allow for the introduction of precise amino acid changes without affecting the overall  $\beta$ -sheet alignment, because all adjacent  $\beta$ -strands are covalently connected.

Biancalana et al. [46] designed a minimalist ThT binding site in the PSAMs using the combined principles established through computational

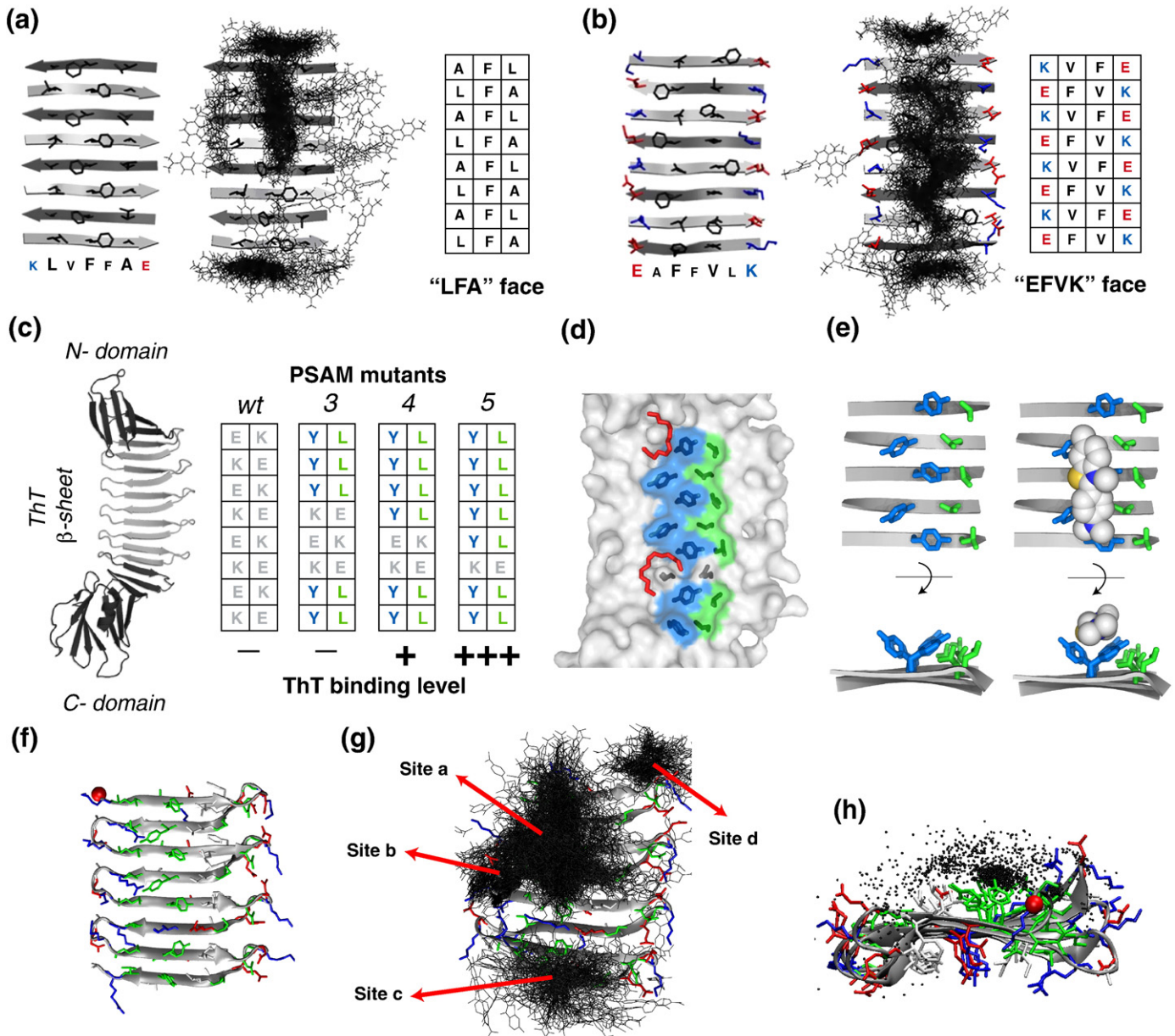


**Fig. 4.** Atomic resolution investigations of ThT binding sites and ThT- $\beta$ -sheet interactions. (a and b) Binding of ThT to the KLVFFAE protofibril probed using molecular dynamics simulations [45]. Only the  $\beta$ -sheet faces of the protofibril are shown, since ThT did not appreciably bind between the laminated  $\beta$ -sheets. (a) Binding of ThT to the "LFA" face of the protofibril  $\beta$ -sheet. The structure of the starting structure is shown at left, with the bottom  $\beta$ -strand labeled to distinguish side chains in the front (large letters) and back (small letters) of the  $\beta$ -sheet. The clustered populations of bound ThT molecules are shown at center. The amino acid identities of the "LFA" side-chain ladders on this face are shown at right. Side chains are colored blue for positive, red for negative, and black for hydrophobic. The backbone is shown in cartoon representation [45]. (b) Binding of ThT to the "EFVK"  $\beta$ -sheet face of the protofibril, shown as in (a). (c) Crystal structure of the peptide self-assembly mimic (PSAM) scaffold showing the central  $\beta$ -sheet capped by N- and C-terminal domains (PDB 3EC5) [46]. The amino acid identities of the wild-type cross-strand ladders are shown, as well as the designed ladders in the 3-YY/LL, 4-YY/LL, and 5-YY/LL mutants. The relative strength of the interactions of these PSAMs with ThT (as determined by fluorescence intensity and  $K_d$ ) are indicated below. (d) Magnified view of the ThT-binding  $\beta$ -sheet of the 5-YY/LL PSAM [46]. The amino acid identities of the designed ladders are given in (c). The side chains of the designed residues of the ThT binding site as shown as sticks. These residues and their solvent-exposed surfaces are colored blue for Tyr and green for Leu, while wild-type side chains are in dark gray. The two PEG-400 molecules found near the ThT-binding site are shown as red sticks. (e) The side-chain conformations of the PSAM ladders implicated in ThT-binding [46]. The ladders are shown looking down the long axis of the PSAM from C- to N-terminus (top) and looking straight down on the  $\beta$ -sheet (bottom). The backbone is depicted in cartoon form, with turns omitted for clarity. At the right is shown a binding orientation for ThT determined by molecular dynamics simulation [50]. The carbon, nitrogen and sulfur elements of ThT are in white, blue, and yellow, respectively. (f) The  $\beta$ -sheet segment of the PSAM used for molecular dynamics simulations of ThT binding [50]. The N- and C-terminal domains were omitted to reduce the computational cost, as these domains have been experimentally demonstrated not to bind ThT. Aromatic residues are shown in green, hydrophobic residues are gray, positively charged residues are blue, and negatively charged residues are red. (g) Binding modes of ThT within an engineered channel [50]. Four clusters are located at: the shallow groove formed by continuous Tyr side chains (Site a); on top of  $\beta$ -strands 3–5 (Site b) and at the two edges of the  $\beta$ -sheet (Sites c and d). ThT molecules are represented by lines. Site a is the most populated and energetically favored of these sites, and precisely corresponds to the engineered ThT-binding mutations. (h) Lateral view of the ThT-binding simulation to the PSAM, showing that ThT binds primarily to the designed aromatic-hydrophobic face of the  $\beta$ -sheet [50]. Almost no binding is observed on the opposite charged surface of the  $\beta$ -sheet (each black dot represents a ligand). The N-terminus of the  $\beta$ -sheet is shown as a red ball. Images in all panels have been reproduced with permission.

and macroscopic analysis of ThT interactions (Fig. 4c). The wild-type PSAM contains a series of highly charged amino acid ladders and it was found not to appreciably bind ThT, in agreement with the poor affinity of

ThT for many highly charged fibrils [31,48] (Fig. 4c). Systematic mutagenesis allowed the introduction of a series of cross-strand ladders containing hydrophobic and aromatic amino acids (Fig. 4c), which are

commonly found in fibril-forming peptides [33,49] and were observed as a principal ThT binding site in simulations [44]. Ultimately, adjacent (side-by-side) ladders formed from Tyr and Leu generated a high-affinity ( $K_d \sim 2 \mu\text{M}$ ) ThT binding site that recapitulated all hallmarks of ThT binding to fibrils, including intense fluorescence and the Cotton effect (Fig. 4d and e). Moreover, stoichiometric analysis demonstrated that ThT bound to the Tyr-Leu site as a single, discrete molecule, as opposed to a micelle or a dimer.

The crystal structure of the ThT-binding PSAM in the absence of ThT revealed a shallow groove formed by alternating conformers of Tyr aromatic rings, stabilized by packing interactions with adjacent Leu residues (Fig. 4d and e). Unfortunately, apparent direct competition between ThT and the polyethylene glycol (PEG) used for crystallization prevented visualization of ThT interactions with the  $\beta$ -sheet surface (Fig. 4d).

Subsequent molecular dynamics analysis of the PSAM in the presence of ThT enabled the first application of dye-binding simulations to a discrete and well-defined ThT binding site [50]. The hybrid experimental and computational approach employed to study the PSAMs has thus provided an important link between dye-binding simulations and experimentally testable hypotheses. Molecular dynamics simulations were conducted in a similar manner as for the eight-stranded KLVFFAE protofibrils described above [44,45]. In order to maximize computational efficiency, the N- and C-terminal globular domains of the PSAMs were removed, as these have been experimentally demonstrated not to bind ThT. The initial system was composed of a periodic water box containing  $\sim 5600$  water molecules, the “excised” PSAM flat  $\beta$ -sheet, two ThT molecules, and two neutralizing chloride ions. Simulations were conducted at 310 K over 100 ns, and the resulting populations of bound ThT molecules were clustered into predominant binding modes. These simulations demonstrated that ThT binds primarily to the designed site along the shallow groove formed by cross-strand Tyr side chains, making subtle contacts with the adjacent Leu ladder (Fig. 4f–h, Site a). The striking similarity between the Val-Phe [44] and Tyr-Leu [50] ThT-binding motifs observed in simulations offers support for the validity and potency of such aromatic-mediated ThT binding modes. These results strongly suggest that surface-exposed channels rich in aromatic amino acids are the primary binding sites of ThT. Together, the findings rationalize the broad binding spectrum of ThT.

### 2.3. Size requirements for ThT binding sites

The PSAM system has been uniquely powerful in defining the minimal size requirements for ThT binding due to the ease with which ThT binding sites of varying sizes can be produced through site-directed mutagenesis. Though recent work has yielded atomic-resolution insight into microcrystalline self-assemblies, which could in principle be used as the starting structure for systematic mutagenesis experiments for ThT binding, the surface properties of the short peptide subunits cannot be precisely manipulated without disrupting, destabilizing or altering the mode of assembly [34,35]. In contrast, because the PSAM scaffold is highly stable and monomeric, point mutations can confidently be used to manipulate a localized and well-defined ThT binding site without altering the overall polypeptide structure. Biancalana et al. [46] determined the minimal binding site for ThT by systematically dissecting a long channel composed of Tyr and Leu into sequentially shorter binding sites (Fig. 4c). The shorter ThT-binding motifs were generated by reverting the Tyr and Leu ladders to the charged amino acid residues (Lys and Glu) found in the wild-type PSAM that exhibited no detectable ThT binding. These experiments suggested that the minimal discrete binding site for ThT is comprised from a channel across five or more  $\beta$ -strands of a flat  $\beta$ -sheet surface (Fig. 4c–e).

The molecular dynamics simulations of ThT binding to the PSAM (Fig. 4g, Site a) have helped generalize the requirements for mini-

malist ThT-binding motifs. The simulations demonstrated that the ThT molecules bound to the PSAM are dispersed by a longitudinal translation across the five Leu and Tyr residues with a magnitude up to the spacing between adjacent  $\beta$ -strands. The lack of a single preferred orientation of ThT within this site indicates that the groove across five cross-strand residue pairs is in actuality slightly longer than the minimal ThT binding site. The head-to-tail length of ThT ( $\sim 15 \text{ \AA}$ ) is in fact closer to the  $\text{C}\alpha$ – $\text{C}\alpha$  distance of a four-residue ladder ( $\sim 14 \text{ \AA}$ ) than a five-residue ladder [46,50]. Although Biancalana et al. have shown that a PSAM containing a similar Tyr-Leu ladder across only four  $\beta$ -strands binds ThT weakly, this effect is likely to have been caused by the charged amino acids used to replace the Tyr and Leu residues. Thus, the results of these simulations suggest that, in the absence of repulsive electrostatic interactions, ThT can bind to a minimal groove formed from four aromatic-hydrophobic cross-strand residues. Because these results establish a minimal structural threshold for high-affinity ThT binding, they should facilitate interpretation of ThT-binding data in molecular terms. Knowledge gained from PSAM studies may therefore be useful for better defining the structure of small self-assemblies and protein oligomers.

The size requirements described above also rationalize why ThT does not bind most  $\beta$ -sheet rich globular proteins. Typical globular proteins contain highly twisted  $\beta$ -sheets consisting of less than four  $\beta$ -strands, which are thus too distorted and too short to form suitable ThT-binding motifs [38,51,52]. However, the self-assembly of native-like proteins can give rise to large fibrillar structures capable of binding ThT [53], such as observed for  $\beta 2$ -microglobulin [54] and transthyretin [55]. Although the  $\beta$ -sheet surfaces found in the native structures of these aggregating proteins are often only three  $\beta$ -strands in width and are thus incapable of binding ThT, when assembled in the context of fibrils, these proteins create extended  $\beta$ -sheet surfaces that form a ThT-binding motif.

### 2.4. Sequence preferences in ThT binding sites

Despite its capacity to bind an extraordinary variety of amyloid [15], ThT possesses some level of amino acid sequence specificity. Identifying amino acid motifs capable of binding ThT has been immeasurably aided by atomic-resolution studies of ThT–fibril interactions, which have demonstrated that the ThT-binding behavior of a fibril often correlates with the chemical properties of particular cross-strand ladders. Many interactions with ThT are mediated predominantly by aromatic side-chains, particularly Tyr and Phe (Figs. 3 and 4) [44–46,50]. Aromatic residues present large hydrophobic surfaces along which ThT can bind, and moreover their capacity to  $\pi$ -stack with the dye may be a key component of many dye-binding interactions. In the case of the PSAMs, even though alternating Tyr conformers formed the majority of the dye-binding site, the Leu ladder (which replaced charged residues) was also critical for generating a strong affinity to ThT [46,50]. These results demonstrate that side-chain interactions in ThT binding sites are likely to be cooperative and sometimes difficult to predict.

Contrarily, a number of general characteristics have also been proposed for fibrils with a poor capacity to bind ThT. The fact that highly charged fibrils such as poly-Lys do not appreciably bind ThT is likely due to electrostatic repulsion [31,48]. Precise point mutagenesis in the PSAM system has moreover demonstrated that charged amino acids are particularly efficient at ablating ThT binding (Fig. 4g) [46,50]. These results are consistent with the observed dependence of ThT affinity on experimental conditions. For instance, the affinity of ThT is lower at acidic pH than at neutral pH, probably due to electrostatic repulsion of the dye by an increase in positive charge [13,31]. Accordingly, the reduction in affinity at acidic pH can be overcome by shielding like charges between the dye and fibril through increasing the ionic strength [12,31]. These considerations have been thoroughly



reviewed elsewhere [15]. Proper interpretation of results obtained through ThT staining thus requires an intimate understanding of the mechanistic basis by which ThT recognizes the structural features of amyloid.

### 2.5. ThT binding to non-fibrillar structures

Despite its demonstrated utility as an amyloid stain, continued concerns over potential cross-reactivity of ThT have led to several important studies probing its specificity. In particular, ThT's capacity to bind hydrophobic pockets in globular proteins has been extensively characterized. The crystal structure of ThT bound to acetylcholinesterase demonstrated that the dye binds in a site formed primarily of  $\alpha$ -helices, in striking contrast to cross- $\beta$  fibrils (Fig. 3) [32]. Interestingly, nearly all contacts with ThT were mediated by aromatic residues in the binding pocket, including extensive  $\pi$ -stacking with Tyr and Trp (Fig. 3b). The structure thus bears a strong resemblance to the Tyr-rich channel of the ThT-binding PSAM, in particular the binding cleft created by orthogonal orientations of the adjacent aromatic rings (Fig. 4e). A model of Congo red bound parallel to the  $\beta$ -strands of a dimer of porcine insulin contained an abundance of interactions between the dye molecule and aromatic side chains, though it should be noted that the dye molecules could be modeled only with an extremely low occupancy of  $\sim 3\%$ , casting a significant doubt on the validity of this structural model [56]. ThT has also been shown to bind to a hydrophobic pocket of human serum albumin with comparable affinity to many drug-like molecules [57]. ThT's capacity to interact with hydrophobic pockets in non-fibrillar proteins may also rationalize its ability to bind in cavities between protomers of insulin fibrils [42,43]. These observations emphasize that it is essential to verify that ThT does not stain the starting materials when used as a fibrillization reporter, especially in cases of fibrils formed from associations of globular proteins.

### 2.6. Implications of atomic models of ThT-binding in the use of amyloid dyes

Taken together, the atomic-level descriptions of the channel model of ThT binding have highlighted a number of important considerations for the use of ThT. It is clear that particular care must be taken when ThT is used in the presence of other amyloid dyes or inhibitors, as these compounds often have overlapping binding sites along the fibril surface, or spectroscopic properties that interfere with interpreting ThT staining. An especially deceptive example is the case of the aromatic antibiotic rifampicin, which completely ablates ThT binding to islet amyloid fibrils without altering their structure [58]. ThT binding has been shown to be inhibited by common reagents such as glycerol [59], PEG [46], and the hydrophobic dye bis-ANS [46], as well as by the polyphenols resveratrol and curcumin [60]. Thus, the dramatic decrease in ThT binding in the presence of these compounds is likely due to direct competition for common binding sites within channels on the fibril surface, rather than the dissociation of the fibrils themselves. As shown by the crystal structure of the ThT-binding PSAM, well-ordered PEG molecules within the cross-strand channel occluded the ThT binding site [46]. Screens for novel amyloid inhibitors must therefore be performed with extreme caution if employing ThT fluorescence as a detection method.

ThT has historically been regarded as a passive amyloid reporter that shows no appreciable influence on the size, morphology, or rate of growth of amyloid fibrils [61–64]. However, the passivity of ThT as an amyloid dye often appears to be assumed rather than demonstrated. Indeed only sparse datasets in a limited number of fibril systems have been used to substantiate the minimal perturbations to amyloid structure induced by the dye [61–64]. Given that ThT bears structural similarity to many amyloid inhibitors in that it contains multiple aromatic rings [15,25,26], it is quite possible that ThT influences fibril formation. Similar compounds such as Congo red have to varying

degrees displayed a capacity to both enhance and inhibit fibril formation [65,66], potentially compromising their objectivity as diagnostic tools. The preferential binding of ThT to  $\beta$ -sheet surfaces also suggests that ThT can interfere with  $\beta$ -sheet lamination necessary for fibril formation. Therefore, further careful studies are required to determine the degree to which ThT influences fibril structure and kinetics.

### 3. Conclusions and future perspectives

For over 50 years, the success of ThT as an amyloid dye has resulted from its broad staining capacity, extraordinary sensitivity, and ease of use. These considerations have made it among the most widely used dyes for monitoring amyloid formation. ThT's robust staining properties continue to form the basis of innovative methods for the detection and analysis of fibrils both *in vitro* and *in vivo*. Further investigations into the molecular mechanism of ThT interactions are needed to advance our understanding of amyloid formation, kinetics, structure, and pathogenesis. Insights from such investigations will assist those who design amyloid probes and those who apply them in research and diagnostic settings. The recent intense study of the molecular mechanism of ThT binding suggests it may be possible to apply structure-guided design to modulate the specificity of ThT to particular amyloid fibrils. Moreover, as a representative amyloid dye, understanding ThT interactions in atomic detail will ultimately guide therapies to treat amyloid diseases.

### Note added in proof

Recent work showed that ThT has antimicrobial effects through a yet-defined mechanism. B. Lakatos, B. Kalinakova, D. Hudecova, L. Varecka, New effects and applications of thioflavins, Central European Journal of Biology, 5 (2010) 143–150.

### Acknowledgments

M. Biancalana thanks the NIH-Cambridge Scholars Program for support.

### References

- [1] C.M. Dobson, Protein folding and misfolding, *Nature* 426 (2003) 884–890.
- [2] Y. Xing, K. Higuchi, Amyloid fibril proteins, *Mech. Ageing Dev.* 123 (2002) 1625–1636.
- [3] R. Virchow, Nouvelles observations sur la substance animale analogue a la cellulose vegetale, *C.R. Acad. Sci. (Paris)* 37 (1853) 860–861.
- [4] K. Aterman, A historical note on the iodine-sulphuric acid reaction of amyloid, *Histochemistry* 49 (1976) 131–143.
- [5] A.J. Howie, D.B. Brewer, D. Howell, A.P. Jones, Physical basis of colors seen in Congo red-stained amyloid in polarized light, *Lab. Invest.* 88 (2008) 232–242.
- [6] M.T. Elghetany, A. Saleem, Methods for staining amyloid in tissues: a review, *Stain Technol.* 63 (1988) 201–212.
- [7] P.S. Vassar, C.F. Culling, Fluorescent stains, with special reference to amyloid and connective tissues, *Arch. Pathol.* 68 (1959) 487–498.
- [8] H. Naiki, K. Higuchi, M. Hosokawa, T. Takeda, Fluorometric determination of amyloid fibrils in vitro using the fluorescent dye, thioflavin T, *Anal. Biochem.* 177 (1989) 244–249.
- [9] H. Naiki, K. Higuchi, K. Matsushima, A. Shimada, W.H. Chen, M. Hosokawa, T. Takeda, Fluorometric examination of tissue amyloid fibrils in murine senile amyloidosis: use of the fluorescent indicator, thioflavine T, *Lab. Invest.* 62 (1990) 768–773.
- [10] H. Naiki, K. Higuchi, K. Nakakuki, T. Takeda, Kinetic analysis of amyloid fibril polymerization in vitro, *Lab. Invest.* 65 (1991) 104–110.
- [11] H. LeVine III, Thioflavine T interaction with synthetic Alzheimer's disease beta-amyloid peptides: detection of amyloid aggregation in solution, *Protein Sci.* 2 (1993) 404–410.
- [12] H. LeVine III, Stopped-flow kinetics reveal multiple phases of thioflavin T binding to Alzheimer beta (1–40) amyloid fibrils, *Arch. Biochem. Biophys.* 342 (1997) 306–316.
- [13] H. LeVine III, Thioflavine T interaction with amyloid beta-sheet structures, *Amyloid* 2 (1995) 1–6.
- [14] M. Lindgren, K. Sorgjerd, P. Hammarstrom, Detection and characterization of aggregates, prefibrillar amyloidogenic oligomers, and protofibrils using fluorescence spectroscopy, *Biophys. J.* 88 (2005) 4200–4212.
- [15] M. Groenning, Binding mode of Thioflavin T and other molecular probes in the context of amyloid fibrils—current status, *J. Chem. Biol.* (2009).
- [16] R. Nelson, D. Eisenberg, Recent atomic models of amyloid fibril structure, *Curr. Opin. Struct. Biol.* 16 (2006) 260–265.

- [17] O.S. Makin, L.C. Serpell, Structures for amyloid fibrils, *FEBS J.* 272 (2005) 5950–5961.
- [18] L. Goldschmidt, P.K. Teng, R. Riek, D. Eisenberg, Identifying the amyloids, proteins capable of forming amyloid-like fibrils, *Proc. Natl. Acad. Sci. U. S. A.* 107 (2010) 3487–3492.
- [19] D.M. Fowler, A.V. Koulov, W.E. Balch, J.W. Kelly, Functional amyloid—from bacteria to humans, *Trends Biochem. Sci.* 32 (2007) 217–224.
- [20] S.K. Maji, M.H. Perrin, M.R. Sawaya, M.L. Debnath, K. Vadodaria, R.A. Rissman, P.S. Singru, K.P. Nilsson, R. Simon, D. Schubert, D. Eisenberg, J. Rivier, P. Sawchenko, W. Vale, R. Riek, Functional amyloids as natural storage of peptide hormones in pituitary secretory granules, *Science* 325 (2009) 328–332.
- [21] C.B. Andersen, H. Yagi, M. Manno, V. Martorana, T. Ban, G. Christiansen, D.E. Otzen, Y. Goto, C. Rischel, Branching in amyloid fibril growth, *Biophys. J.* 96 (2009) 1529–1536.
- [22] L. Cai, R.B. Innis, V.W. Pike, Radioligand development for PET imaging of beta-amyloid (A $\beta$ )—current status, *Curr. Med. Chem.* 14 (2007) 19–52.
- [23] W.E. Klunk, Y. Wang, G.F. Huang, M.L. Debnath, D.P. Holt, C.A. Mathis, Uncharged thioflavin-T derivatives bind to amyloid-beta protein with high affinity and readily enter the brain, *Life Sci.* 69 (2001) 1471–1484.
- [24] W.E. Klunk, H. Engler, A. Nordberg, Y. Wang, G. Blomqvist, D.P. Holt, M. Bergstrom, I. Savitcheva, G.F. Huang, S. Estrada, B. Aussen, M.L. Debnath, J. Barletta, J.C. Price, J. Sandell, B.J. Lopresti, A. Wall, P. Koivisto, G. Antoni, C.A. Mathis, B. Langstrom, Imaging brain amyloid in Alzheimer's disease with Pittsburgh Compound-B, *Ann. Neurol.* 55 (2004) 306–319.
- [25] Y. Kim, J.H. Lee, J. Ryu, D.J. Kim, Multivalent & multifunctional ligands to beta-amyloid, *Curr. Pharm. Des.* 15 (2009) 637–658.
- [26] K.P. Nilsson, Small organic probes as amyloid specific ligands—past and recent molecular scaffolds, *FEBS Lett.* 583 (2009) 2593–2599.
- [27] W. Dzwolak, M. Pecul, Chiral bias of amyloid fibrils revealed by the twisted conformation of Thioflavin T: an induced circular dichroism/DFT study, *FEBS Lett.* 579 (2005) 6601–6603.
- [28] A. Loksztajn, W. Dzwolak, Chiral bifurcation in aggregating insulin: an induced circular dichroism study, *J. Mol. Biol.* 379 (2008) 9–16.
- [29] V.I. Stsiapura, A.A. Maskevich, V.A. Kuzmitsky, K.K. Turoverov, I.M. Kuznetsova, Computational study of thioflavin T torsional relaxation in the excited state, *J. Phys. Chem. A* 111 (2007) 4829–4835.
- [30] E.S. Voropai, Spectral properties of Thioflavin T and its complexes with amyloid fibrils, *J. Appl. Spectrosc.* 70 (2003) 868–874.
- [31] R. Sabate, I. Lascu, S.J. Saupé, On the binding of Thioflavin-T to HET-s amyloid fibrils assembled at pH 2, *J. Struct. Biol.* 162 (2008) 387–396.
- [32] M. Harel, L.K. Sonoda, I. Silman, J.L. Sussman, T.L. Rosenberry, Crystal structure of thioflavin T bound to the peripheral site of *Torpedo californica* acetylcholinesterase reveals how thioflavin T acts as a sensitive fluorescent reporter of ligand binding to the acylation site, *J. Am. Chem. Soc.* 130 (2008) 7856–7861.
- [33] M. Biancalana, K. Makabe, A. Koide, S. Koide, Aromatic cross-strand ladders control the structure and stability of beta-rich peptide self-assembly mimics, *J. Mol. Biol.* 383 (2008) 205–213.
- [34] R. Nelson, M.R. Sawaya, M. Balbirnie, A.O. Madsen, C. Riekel, R. Grothe, D. Eisenberg, Structure of the cross-beta spine of amyloid-like fibrils, *Nature* 435 (2005) 773–778.
- [35] M.R. Sawaya, S. Sambashivan, R. Nelson, M.I. Ivanova, S.A. Sievers, M.I. Apostol, M.J. Thompson, M. Balbirnie, J.J. Wiltzius, H.T. McFarlane, A.O. Madsen, C. Riekel, D. Eisenberg, Atomic structures of amyloid cross-beta spines reveal varied steric zippers, *Nature* 447 (2007) 453–457.
- [36] O.S. Makin, E. Atkins, P. Sikorski, J. Johansson, L.C. Serpell, Molecular basis for amyloid fibril formation and stability, *Proc. Natl. Acad. Sci. U. S. A.* 102 (2005) 315–320.
- [37] T. Sato, P. Kienlen-Campard, M. Ahmed, W. Liu, H. Li, J.I. Elliott, S. Aimoto, S.N. Constantinescu, J.N. Octave, S.O. Smith, Inhibitors of amyloid toxicity based on beta-sheet packing of A $\beta$ 40 and A $\beta$ 42, *Biochemistry* 45 (2006) 5503–5516.
- [38] M.R. Krebs, E.H. Bromley, A.M. Donald, The binding of thioflavin-T to amyloid fibrils: localisation and implications, *J. Struct. Biol.* 149 (2005) 30–37.
- [39] J.H. Cooper, Selective amyloid staining as a function of amyloid composition and structure. Histochemical analysis of the alkaline Congo red, standardized toluidine blue, and iodine methods, *Lab. Invest.* 31 (1974) 232–238.
- [40] G.G. Glenner, E.D. Eanes, H.A. Bladen, R.P. Linke, J.D. Termini, Beta-pleated sheet fibrils. A comparison of native amyloid with synthetic protein fibrils, *J. Histochem. Cytochem.* 22 (1974) 1141–1158.
- [41] R. Khurana, C. Coleman, C. Ionescu-Zanetti, S.A. Carter, V. Krishna, R.K. Grover, R. Roy, S. Singh, Mechanism of thioflavin T binding to amyloid fibrils, *J. Struct. Biol.* 151 (2005) 229–238.
- [42] M. Groenning, L. Olsen, M. van de Weert, J.M. Flink, S. Frokjaer, F.S. Jorgensen, Study on the binding of Thioflavin T to beta-sheet-rich and non-beta-sheet cavities, *J. Struct. Biol.* 158 (2007) 358–369.
- [43] M. Groenning, M. Norrman, J.M. Flink, M. van de Weert, J.T. Bukrinsky, G. Schluckebier, S. Frokjaer, Binding mode of Thioflavin T in insulin amyloid fibrils, *J. Struct. Biol.* 159 (2007) 483–497.
- [44] C. Wu, Z. Wang, H. Lei, W. Zhang, Y. Duan, Dual binding modes of Congo red to amyloid protofibril surface observed in molecular dynamics simulations, *J. Am. Chem. Soc.* 129 (2007) 1225–1232.
- [45] C. Wu, Z. Wang, H. Lei, Y. Duan, M.T. Bowers, J.E. Shea, The binding of thioflavin T and its neutral analog BTA-1 to protofibrils of the Alzheimer's disease A $\beta$ 25 (16–22) peptide probed by molecular dynamics simulations, *J. Mol. Biol.* 384 (2008) 718–729.
- [46] M. Biancalana, K. Makabe, A. Koide, S. Koide, Molecular mechanism of Thioflavin-T binding to the surface of beta-rich peptide self-assemblies, *J. Mol. Biol.* 385 (2009) 1052–1063.
- [47] K. Makabe, D. McElheny, V. Tereshko, A. Hilyard, G. Gawlak, S. Yan, A. Koide, S. Koide, Atomic structures of peptide self-assembly mimics, *Proc. Natl. Acad. Sci. U. S. A.* 103 (2006) 17753–17758.
- [48] R. Khurana, C. Ionescu-Zanetti, M. Pope, J. Li, L. Nielson, M. Ramirez-Alvarado, L. Regan, A.L. Fink, S.A. Carter, A general model for amyloid fibril assembly based on morphological studies using atomic force microscopy, *Biophys. J.* 85 (2003) 1135–1144.
- [49] E. Gazit, Mechanisms of amyloid fibril self-assembly and inhibition. Model short peptides as a key research tool, *FEBS J.* 272 (2005) 5971–5978.
- [50] C. Wu, M. Biancalana, S. Koide, J.E. Shea, Binding modes of Thioflavin-T to the single-layer beta-sheet of the peptide self-assembly mimics, *J. Mol. Biol.* (2009).
- [51] C. Chothia, Conformation of twisted beta-pleated sheets in proteins, *J. Mol. Biol.* 75 (1973) 295–302.
- [52] J.S. Richardson, D.C. Richardson, Natural beta-sheet proteins use negative design to avoid edge-to-edge aggregation, *Proc. Natl. Acad. Sci. U. S. A.* 99 (2002) 2754–2759.
- [53] F. Chiti, C.M. Dobson, Amyloid formation by globular proteins under native conditions, *Nat. Chem. Biol.* 5 (2009) 15–22.
- [54] H. Benyamini, K. Gunasekaran, H. Wolfson, R. Nussinov, beta(2)-microglobulin amyloidosis: insights from conservation analysis and fibril modelling by protein docking techniques, *J. Mol. Biol.* 330 (2003) 159–174.
- [55] A.A. Serag, C. Altenbach, M. Gingery, W.L. Hubbell, T.O. Yeates, Arrangement of subunits and ordering of beta-strands in an amyloid sheet, *Nat. Struct. Biol.* 9 (2002) 734–739.
- [56] W.G. Turnell, J.T. Finch, Binding of the dye congo red to the amyloid protein pig insulin reveals a novel homology amongst amyloid-forming peptide sequences, *J. Mol. Biol.* 227 (1992) 1205–1223.
- [57] P. Sen, S. Fatima, B. Ahmad, R.H. Khan, Interactions of thioflavin T with serum albumins: spectroscopic analyses, *Spectrochim. Acta A Mol. Biomol. Spectrosc.* 74 (2009) 94–99.
- [58] F. Meng, P. Marek, K.J. Potter, C.B. Verchere, D.P. Raleigh, Rifampicin does not prevent amyloid fibril formation by human islet amyloid polypeptide but does inhibit fibril thioflavin-T interactions: implications for mechanistic studies of beta-cell death, *Biochemistry* 47 (2008) 6016–6024.
- [59] J. Ryu, M. Kanapathipillai, G. Lentzen, C.B. Park, Inhibition of beta-amyloid peptide aggregation and neurotoxicity by alpha-D-mannosylglycerate, a natural extremolyte, *Peptides* 29 (2008) 578–584.
- [60] S.A. Hudson, H. Ecroyd, T.W. Kee, J.A. Carver, The thioflavin T fluorescence assay for amyloid fibril detection can be biased by the presence of exogenous compounds, *FEBS J.* 276 (2009) 5960–5972.
- [61] L. Nielsen, R. Khurana, A. Coats, S. Frokjaer, J. Brange, S. Vyas, V.N. Uversky, A.L. Fink, Effect of environmental factors on the kinetics of insulin fibril formation: elucidation of the molecular mechanism, *Biochemistry* 40 (2001) 6036–6046.
- [62] V. Fodera, F. Librizzi, M. Groenning, M. van de Weert, M. Leone, Secondary nucleation and accessible surface in insulin amyloid fibril formation, *J. Phys. Chem. B* 112 (2008) 3853–3858.
- [63] M. Mauro, E.F. Craparo, A. Podesta, D. Bulone, R. Carrotta, V. Martorana, G. Tiana, P.L. San Biagio, Kinetics of different processes in human insulin amyloid formation, *J. Mol. Biol.* 366 (2007) 258–274.
- [64] V. Heiser, E. Scherzinger, A. Boeddrich, E. Nordhoff, R. Lurz, N. Schugardt, H. Lehrach, E.E. Wanker, Inhibition of huntingtin fibrillogenesis by specific antibodies and small molecules: implications for Huntington's disease therapy, *Proc. Natl. Acad. Sci. U. S. A.* 97 (2000) 6739–6744.
- [65] Y. Porat, A. Abramowitz, E. Gazit, Inhibition of amyloid fibril formation by polyphenols: structural similarity and aromatic interactions as a common inhibition mechanism, *Chem. Biol. Drug Des.* 67 (2006) 27–37.
- [66] C. Lendel, C.W. Bertoncini, N. Cremades, C.A. Waudby, M. Vendruscolo, C.M. Dobson, D. Schenk, J. Christodoulou, G. Toth, On the mechanism of nonspecific inhibitors of protein aggregation: dissecting the interactions of alpha-synuclein with Congo red and Lacmoid, *Biochemistry* 48 (2009) 8322–8334.